THE UNIVERSITY OF MICHIGAN
COLLEGE OF ENGINEERING
Department of Electrical & Computer Engineering
Space Physics Research Laboratory

A FEASIBILITY STUDY OF A ROCKET-BORNE CHEMILUMINESCENT NITRIC OXIDE DETECTOR

Prepared on behalf of the project by

Conrad J. Mason

under contract with:

National Aeronautics and Space Administration
Goddard Space Flight Center
Contract No. NAS5-21914
Greenbelt, Maryland

administered through:

OFFICE OF RESEARCH ADMINISTRATION ANN ARBOR

June 1973

ABSTRACT

A feasibility study concerning the possible use of a chemiluminescent nitric oxide detector to measure ambient nitric oxide concentrations in the upper atmosphere is described. The topics considered include the significance and need for nitric oxide measurements in the upper atmosphere, theoretical nitric oxide profiles, the theory of a chemiluminescent detector, and a detailed discussion of a proposed rocket-borne chemiluminescent probe. The major conclusion is that such an instrument is feasible. Its ultimate sensitivity and dynamic range render nitric oxide concentrations in the altitude interval 30 to 80 kilometers measurable, in theory.

ACKNOWLEDGMENTS

The author gratefully acknowledges the able assistance of Mr. Jack J. Horvath, who performed the theoretical calculations relating to the flow rate in the sample flow tube. He would also like to express his gratitude to Dr. Donald H. Stedman for his helpful suggestions.

This work was performed under contract NAS5-21914.

TABLE OF CONTENTS

LIST OF ILLUSTRATIONS

1. INTRODUCTION

As yet, no direct measurements of the nitric oxide concentration in the altitude range from 30 km to 80 km have been made; however, a clear need for a precise determination of the variation of nitric oxide density with altitude exists. The importance of nitric oxide to D-region chemistry and the possible formulation of a negative-ion model have been cited by some interested in the measurement capability. Others have suggested that such measurements might provide a possible explanation of the winter D-region anomaly.

The recent development of chemilumescent detectors to measure directly NO concentrations in the parts-per-billion range may provide a means of making the necessary direct measurements in the atmosphere. The primary purpose of this study is to determine if it is indeed feasible to adapt such an instrument to this end.

The topics to be considered in this report are a brief synopsis of the significance and need for nitric oxide measurements in the upper atmosphere; a presentation of several theoretical nitric oxide profiles; a presentation of the theory governing the design and operation of a chemiluminescent detector; a detailed discussion of a proposed rocket-borne chemiluminescent probe including comments relating to the sample flow tube, the reaction chamber, the ozone source, and the photomultiplier. The response of the hypothetical instrument to a postulated NO model atmosphere will also be investigated.

2. SIGNIFICANCE AND NEED

Nitric oxide is an important minor constituent of the upper atmosphere. Not only does it provide the source for D-region ionization under quiet conditions, it also has a large role in the ion chemistry of the lower ionosphere. Furthermore, as a result of its long photochemical lifetime, atmospheric dynamic processes can affect its distribution. To enhance our understanding of these phenomena, it is important to measure the NO concentration as a function of altitude under various atmospheric conditions. For example, ion-pair production in the middle portion of the D-region is caused in part by Lyman-α ionization of NO.[1] Both the Lyman-α flux and the ionization cross section are fairly well known, but a measurement of the NO concentration profile has yet to be determined for a quantitative evaluation of ion-pair production.

In D-region chemistry several minor neutral constituents determine the electron production and loss processes. Among these, NO is important because it undergoes fast charge-transfer reactions with ions of major atmospheric constituents. As Strobel notes, one current problem in D-region chemistry is the large theoretical production rate of NO^+ which leads to electron densities about 10 times greater than observed. Of all the input parameters required for this calculation, the NO concentration is the most uncertain.[2] Also, in an earlier work Strobel finds that the NO distribution in the mesosphere is very sensitive to lower flux boundary conditions, and he calls for a quantitative study of the removal rate in the lower atmosphere.[3] For both of these problems, good measurements of the NO concentration over an appropriate altitude interval are needed.

The problems of ion chemistry extend into the negative-ion domain. In 1969, Working Group 11 on Ion Chemistry of the D- and E-Regions (ICSU) issued the following statement and recommendation:

"... the major obstacle to the formulation of a theoretical negative-ion model arises from the lack of information concerning a) concentrates of the minor constituents, and b) the negative-ion concentrations with which to compare such a model. We recommend that efforts be made to develop techniques to determine the concentration of these constituents (which include NO) and their variations with time and latitude."[4]

Of the minor constituents in the D-region, both atomic oxygen and nitric oxide have long photochemical lifetimes; as a result, atmospheric dynamic processes can affect their distributions. It is these processes that interest those studying the "winter D anomaly," i.e., periods of time when the electron densities in the D-region have anomalously high values for the other prevailing conditions. One way in which meteorological processes can bring about an increase in electron density is simply to effect an increase in the NO concentration; photoionization by Lyman-α would then lead to an increased electron density. However, Sechrist has suggested that the same effect can be brought about by a mesospheric warming.[5] Others have postulated transient planetary wave systems as being responsible.[6,7] Gregory and Manson concluded that various dynamic processes act on certain winter days at middle latitudes to redistribute ionizable constituents in the D-region.[8] However, Geller and Sechrist have recently concluded that the measured increases were due to a decrease in electron-loss efficiency which, in turn, is related to the relative abundances of hydrated positive ions above 80 km.[9] In order to resolve the controversy, the latter authors stated:

"Certainly further coordinated rocket experiments should be carried out on normal and anomalous winter days. Essential parameters to be measured would be electron density, wind and temperature, NO concentration, positive ion density and composition, and precipitating electron flux."

As a matter of record, Working Group 11 has made many recommendations in the last few years that the concentration of NO should be measured at different locations and times under both normal and anomalous conditions. As early as 1968 they recommended that new types of sensors be developed to measure directly important minor constituent concentrations in the altitude range from 50 to 160 km.[10] In 1969 it was stated

> "It is important to make many more measurements, both with existing and new techniques, of the NO profiles under various conditions. These would include various times of day, latitudes, and different seasons as well as during disturbed conditions such as winter anomalies. In this way, it will be possible to determine NO profiles, their systematic variations and the degree of variability."[4]

Once the processes which determine the time and space variations of NO are understood, the study of these variations should provide information on other constituents and also possibly on dynamic processes. Very recently, Bowhill stated:

> "Measurements of minor neutral constituents by a range of techniques should be encouraged, both with rockets and satellites, in order to examine the spatial and temporal variations of these constituents. These measurements should extend downward to the stratosphere."[11]

The measurement of NO concentration in the altitude range 60-120 km has been done by Barth (1966),[12] Pearce (1969),[13] and Meira (1971).[14] In each instance scanning ultraviolet spectrometers were used. Because of some difficulties in interpreting the results of Barth and of Pearce, Working Group 11 said it seemed important to look for alternate ways of measuring NO.[4] Later in the same year, they issued recommendations on rocket measurements which included the statement:

> "The only measurements of nitric oxide carried out to date used optical techniques; more experiments of this type are needed and the development of other direct measurement techniques is encouraged."[15]

Although Meira's subsequent work represents the best effort to date, as he himself notes he used the same optical instrument. As a result, the situation is unchanged today.

Consequently, we find a strong need in several areas of current aeronomical interest for direct measurements of nitric oxide concentrations under a variety of conditions. Recently, a new instrument, the chemiluminescent NO detector, has been developed. The mechanism of the chemiluminescent reaction between NO and ozone was studied definitively by Clough and Thrush in 1966.[16] Not until 1970 did feasibility studies establish that NO detectors based on the chemiluminescent method would work, at least for ground-based operations.[17,18] A 1971 paper by Stedman et al. describes such an instrument and its use as an in situ NO or O_3 detector for photochemical smog studies.[19] With respect to upper atmosphere operation, Ridley et al. very recently (1972) described a series of experiments whose objective is the development of a balloon-borne chemiliminescent NO detector.[20] The following section describes the theory of operation of the chemiluminescent NO detector.

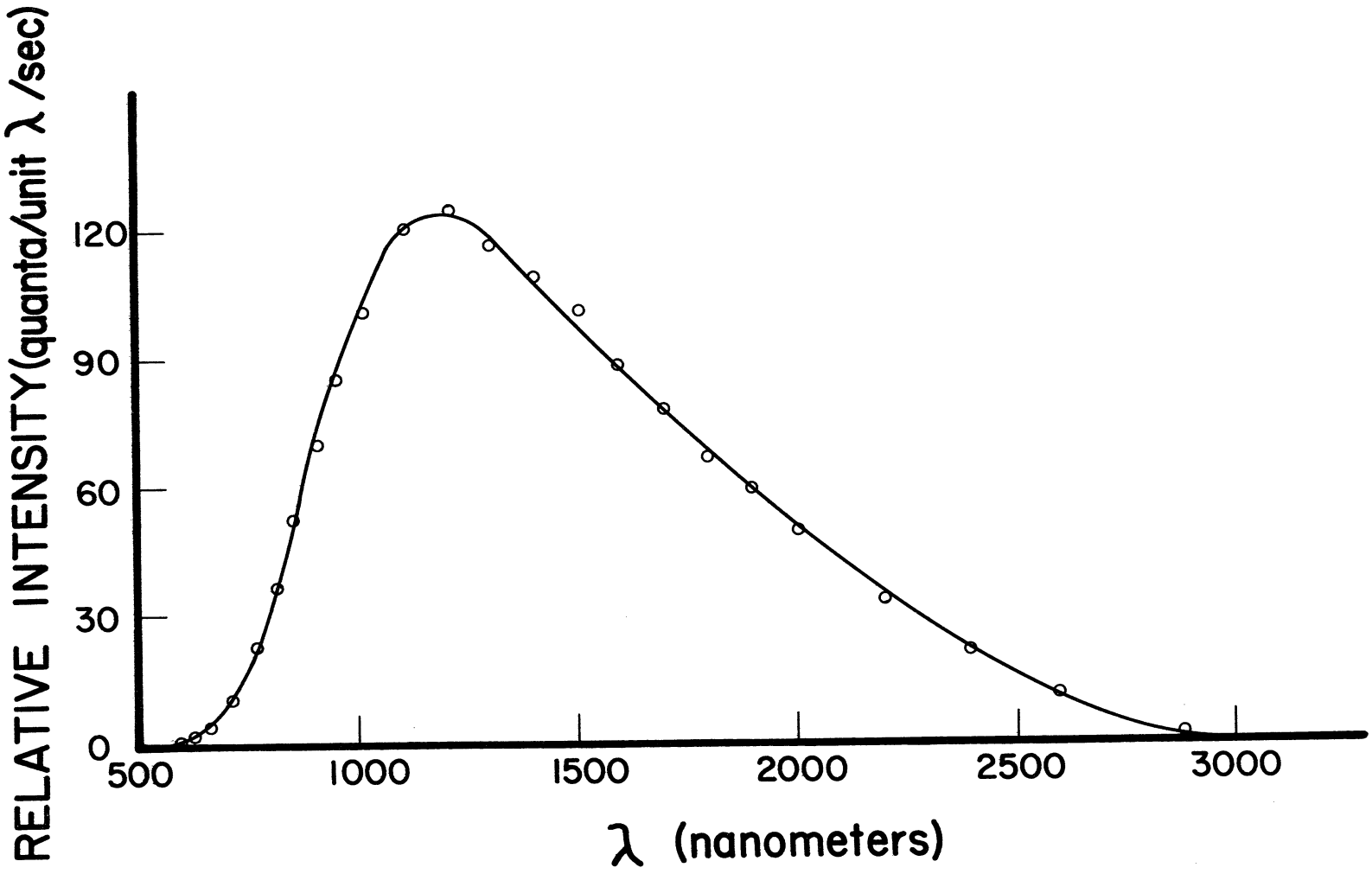

Figure 1. Relative intensity of emitted radiation versus wavelength.

3. THEORY OF OPERATION

The operation of the chemiluminescent NO detector is based on the detection of the light emitted by electronically excited NO_2 molecules which are formed in the reaction of NO with ozone, namely,

$$NO + O_3 \rightarrow NO_2^* + O_2 \qquad (1)$$

$$NO + O_3 \rightarrow NO_2 + O_2 \qquad (2)$$

Reaction (2) competes with (1) and is, in fact, the dominant process; here, the product NO_2 is in the ground state. The excited NO_2 molecules from reaction (1) undergo subsequent de-excitation by either of the following reactions:

$$NO_2^* \rightarrow NO_2 + h\nu \qquad (3)$$

$$NO_2^* + M_i \rightarrow NO_2 + M_i \qquad (4)$$

Reaction (3) is simply photoemission. Clough and Thrush found that the emitted radiation was spread over the wavelength interval from 0.6 to 3.0 micrometers with a peak at about 1.2 micrometers, as shown in Figure 1.[16] Reaction (4), collisional de-excitation, also occurs; note that M_i can be any molecule. The light emitted in reaction (3) is detected by suitable means (usually a photomultiplier); its appearance indicates the presence of NO.

A schematic diagram of a chemiluminescent NO detector is given in Figure 2. Only the essentials of the sensor are shown. It consists of a flow reactor, an ozone source, a sampling orifice, and a photodetector. Ambient NO enters the sampling port

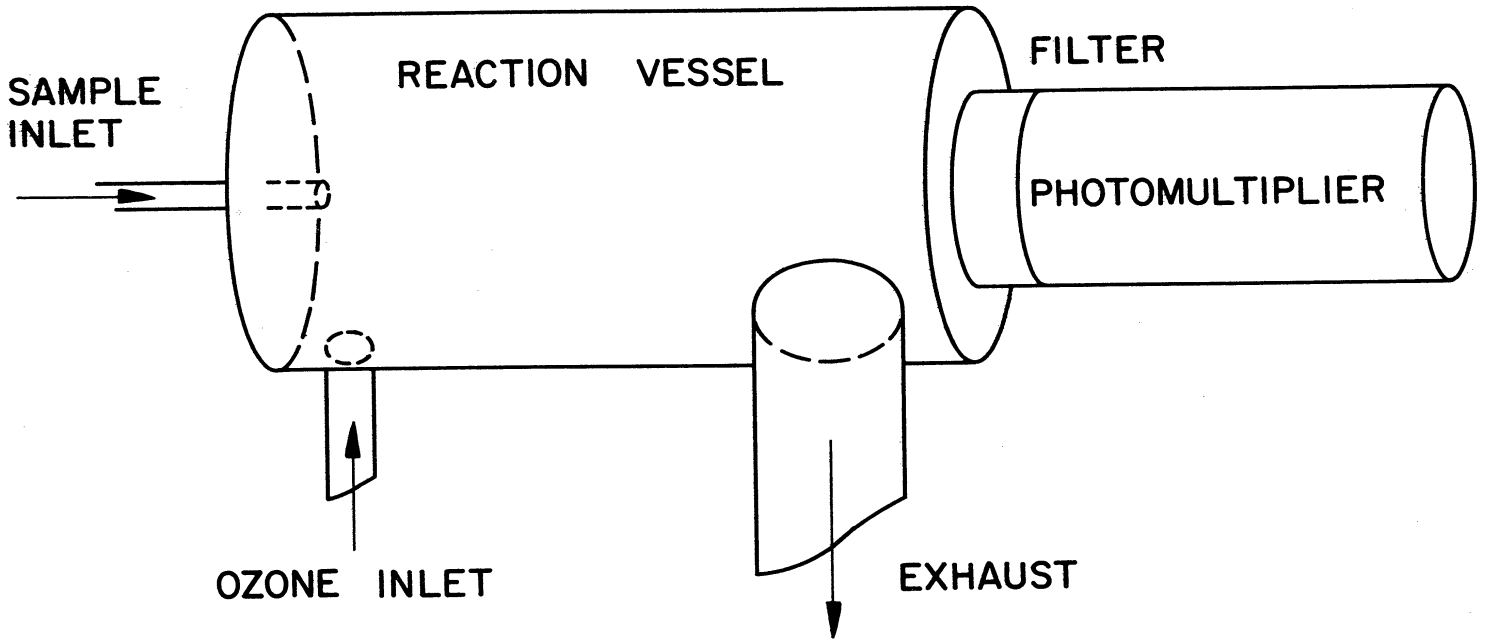

Figure 2. Chemiluminescent nitric oxide detection.

along with other ambient constituents (mostly N_2 and O_2 in this case) and moves to the reactor. Here it reacts with an excess of ozone. The light emitted upon the subsequent de-excitation of NO_2 is detected by a photomultiplier whose output is fed to appropriate signal-conditioning circuitry (n.b., the development that follows parallels that of reference 20 with minor changes in formulation to make it more readily applicable to a higher altitude regime).

If one considers only those four reactions cited above, then the number of photons per second per unit volume is given by

$$I = \frac{k_1 k_3 [O_3][NO]}{k_3 + \sum_i k_i [M_i]} \tag{5}$$

where k_1, k_2, k_3, and k_i are the rate constants corresponding to reactions (1) through (4) (k_1 is the constant for collisional de-excitation by the i^{th} species).

If O_3 is present in excess, then reactions (1) and (2) become psuedo-first order with respect to NO, i.e., the NO concentration as a function of time is given by

$$[NO] = [NO]_{t=0} \exp\{-(k_1 + k_2)[O_3]t\} \tag{6}$$

However, if the reaction volume is a plug-flow reactor with the reactants entering continuously at one end, then the above temporal distribution corresponds to a spatial distribution of NO along the axis of the reactor given by

$$[NO] = [NO]_o \exp\left\{ -(k_1 + k_2)[O_3] \frac{A}{Q} z \right\} \tag{7}$$

where A is the cross-sectional area of the reactor, Q the total volume flow rate, and z the distance down-axis from the reactants' entrance port. $[NO]_o$ is the concentration of NO at this port.

Corresponding to the above axial distribution of NO, the number of photons emitted per second between z and z + dz is given by (from equation 5)

$$I(z)dz = A\frac{k_1k_3[O_3][NO]_o}{k_3 + \sum_i k_i[M_i]} \exp\left\{-(k_1 + k_2)[O_3]\frac{A}{Q}z\right\} dz \qquad (8)$$

The total emission rate is obtained by integrating equation 8 over the length z_o of the reaction volume, i.e.,

$$I_T = A\frac{k_1k_3[NO]_o\, Q}{(k_1 + k_2)(k_3 + \sum_i k_i[M_i])}\left\{1 - \exp\left\{-(k_1 + k_2)[O_3]\frac{A}{Q}z_o\right\}\right\} \qquad (9)$$

Now if z_o is made large so that the exponential term becomes small compared to unity (i.e., the reaction goes to completion in the reactor volume), the above expression reduces to

$$I_T = \frac{k_1k_3[NO]_o\, Q}{(k_1 + k_2)(k_3 + \sum_i k_i[M_i])} \qquad (10)$$

To the extent that $k_3 << \sum_i k_i[M_i]$, and the k_i's are nearly equal, the denominator in equation (10) can be written $(k_1 + k_2)k_i\sum_i[M_i]$; but $\sum_i[M_i]$ is proportional to the total pressure in the reaction volume. Also, $[NO]_o\, Q$ is simply the flux F (molecules per cm^2

per sec) into the reactor. Thus, the absolute intensity is directly proportional to the NO flux, inversely proportional to the pressure in the reactor, and equally as important, independent of the O_3 concentration.

Ridley *et al.*[20] show that the performance of their instruments is in accord with theory in the pressure regime suitable for balloon operations.

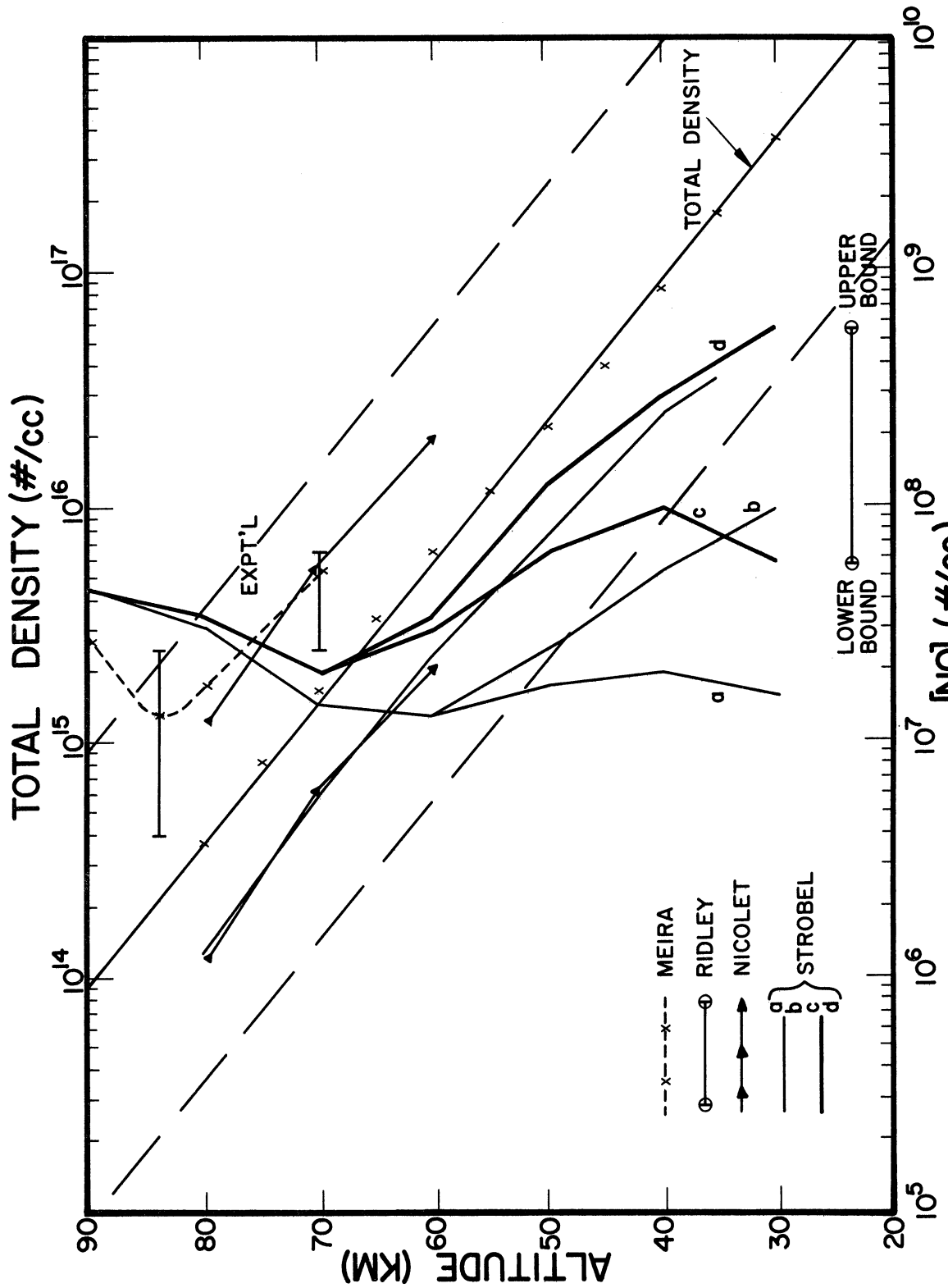

Figure 3. Nitric oxide profiles, measured and theoretical.

4. NITRIC OXIDE PROFILES

At the present time there are no measurements of nitric oxide concentrations from 30 km to 70 km. Very recently Meira carried out some indirect measurements above 70 km.[14] His results indicate a number density of from 2.5×10^7 to 6.5×10^7 molecules cm^{-3} at 70 km and a minimum of about 1.3×10^7 molecules cm^{-3} at 84 km as shown in Figure 3 by the curve labeled "Experimental." Meira's experiment utilized a scanning ultraviolet spectrometer. Although his measurements continue below 70 km, large experimental uncertainties preclude the determination of the NO levels at these altitudes. Even more recently a balloon measurement of the stratospheric NO concentration was made by Ridley et al. with a chemiluminescent detector. Upper and lower bounds of approximately 6×10^8 and 6×10^7 molecules cm^{-3} at an altitude of 23 km have been tentatively established by this experiment.[21] The balloon results are given in Figure 3 as the solid horizontal line at 23 km. To date, these two experiments provide the only measurements of NO levels in our altitude range.

Since actual data are lacking, we must look instead at recent models which purport to give the NO profiles. Nicolet has recently constructed two models[22,23] for the NO concentration and these also are shown in Figure 3. Note that both models have profiles which parallel the total density profile as given by the line labeled "Total Density." Another theoretical model, from Strobel, is also shown in Figure 3; curves labeled "a", "b", "c" and "d" correspond to various lower boundary conditions. His model does show some structure but it is very sensitive to the lower boundary conditions chosen: at 30 km there is an uncertainty of one-and-a-half decades in the predicted concentration. If one were to assume a constant nitric oxide mixing ratio independent of altitude, then its profile would appear as a line

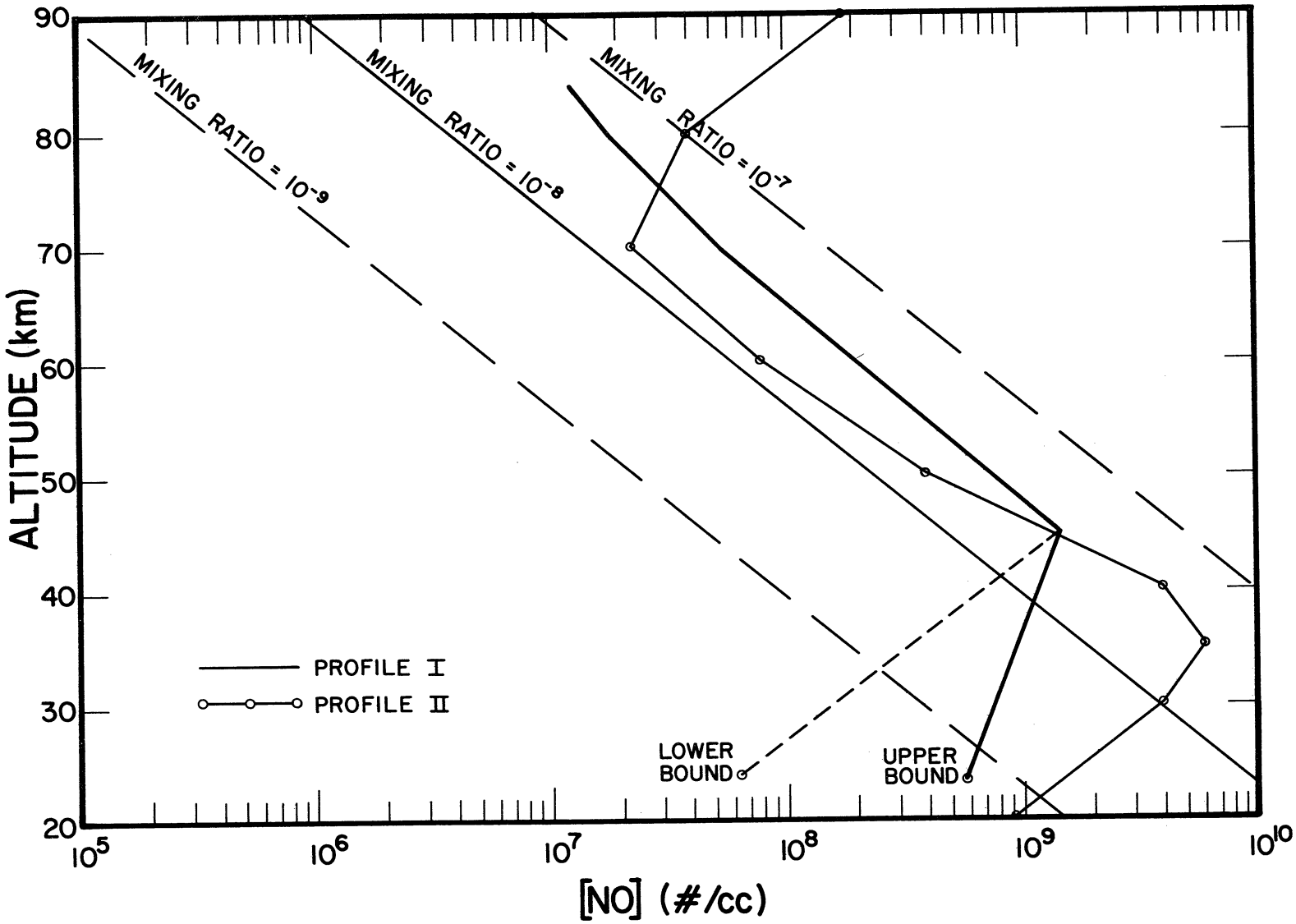

Figure 4. Model nitric oxide profiles.

parallel to the total density profile. Three such lines are pictured in Figure 3: the upper dashed line corresponds to a mixing ratio of 100 parts per billion, the middle solid line to 10 parts per billion, and the lower dashed line to 1 part per billion.

In order to produce a definitive profile with which to compute instrument response, some of the parameters of both the Nicolet and Strobel models have been used to construct a composite model whose features are similar and whose values have been adjusted to fit more closely the experimental values at 23 km and above 70 km. The composite or derived profile is shown in Figure 4 as Profile I. Over most of the altitude range the slope of Profile I is the same as that of the total density profile. At 23 km the value given by the derived model is set equal to Ridley's upper bound. To illustrate uncertainty in concentration at this level a second intercept with his lower bound is also drawn. The composite model produces a conservative estimate of the nitric oxide density.

Very recently Stolarski and Cicerone made an independent assessment of the nitric oxide concentration and derived a model based on that assessment.[24] It also is shown in Figure 4. Their model predicts a maximum NO density at 35 km and is in good agreement with the measurements of Meira.

Also given in Figure 4 are the constant mixing-ratio lines from Figure 3. With these as guides, one can fit his own model by selecting values for the nitric oxide mixing ratio as a function of altitude. The given curves form appropriate bounds for a variation of from 1 part per billion to 100 parts per billion, a range that is sufficient to encompass most educated guesses.

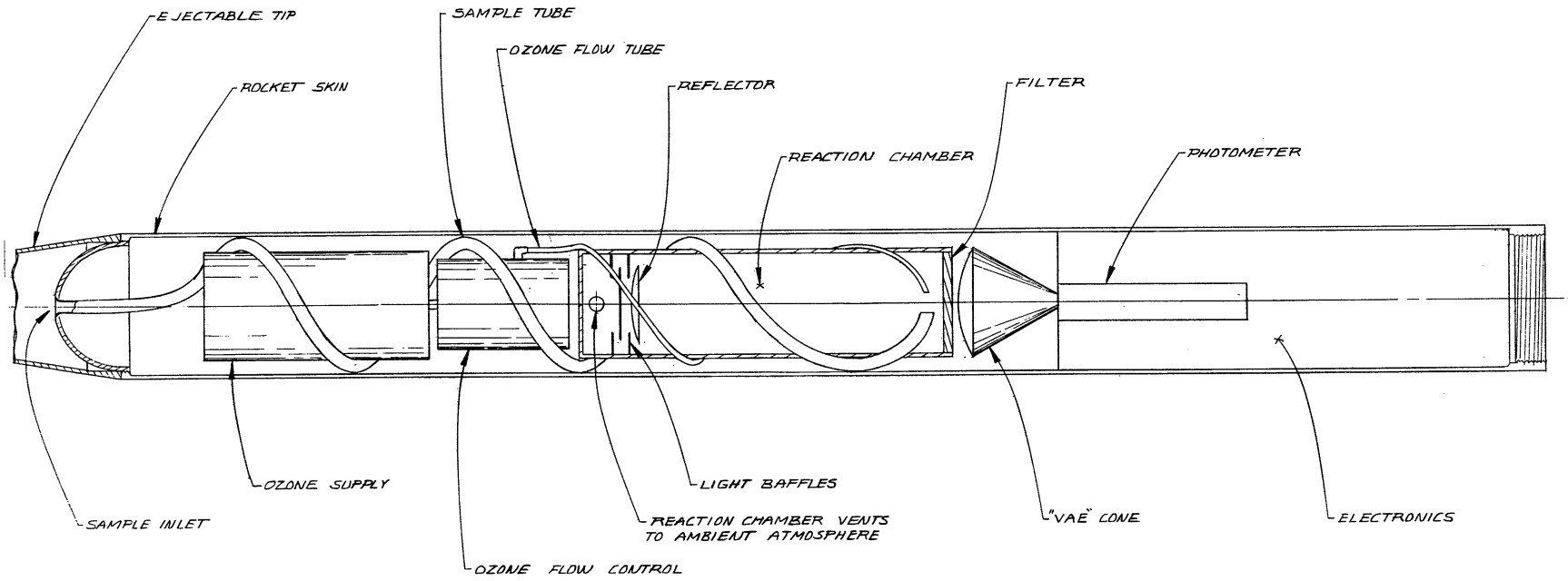

Figure 5. The proposed nitric oxide probe.

5. THE PROPOSED INSTRUMENT

Figure 5 is an illustration of the proposed nitric oxide probe. The ambient sample enters the inlet and moves through the helical flow tube to the reaction chamber. Here it reacts with ozone whose source is the ozone supply bottle and whose concentration in the reaction chamber is determined by the ozone flow control. The emitted radiation from the chemiluminescent reaction passes through a filter and is focused by a simple optical system onto a photomultiplier tube. A reflector at one end of the reaction chamber serves to reflect that radiation away from the photomultiplier. Flow is maintained in the reaction chamber by venting the reacted gases through chamber vents to the ambient atmosphere. Electronic circuitry and batteries are housed in a container at the right end of the probe on the figure. Each of the components sketched in Figure 5 will be considered in more detail in subsequent sections.

The overall dimensions of the proposed instrument are approximately 40 in. in length and 4 in. in diameter. The projected design weight is in the range of from 20 to 25 lb.

5.1. The Sample Flow Tube

The sample inlet is near the stagnation point and behind the bow shock. As a result, the sample is both heated and compressed. Consequently, the flow rate through the sample flow tube depends on the pressure difference between its ends, the stagnation temperature, and the tube size. Preliminary calculations indicate that a tube with a length-to-diameter ratio of about 100 may be satisfactory. For a tube of this nature and in the altitude interval under consideration, all flow regimes are encountered. Initially, the flow is viscous from about 30 km to 65 km; a region of transition flow exists from about 65 km to 75 km; and, finally, near-free-molecular flow prevails from 75 km to 80 km. Because of these changes in the character of the flow,

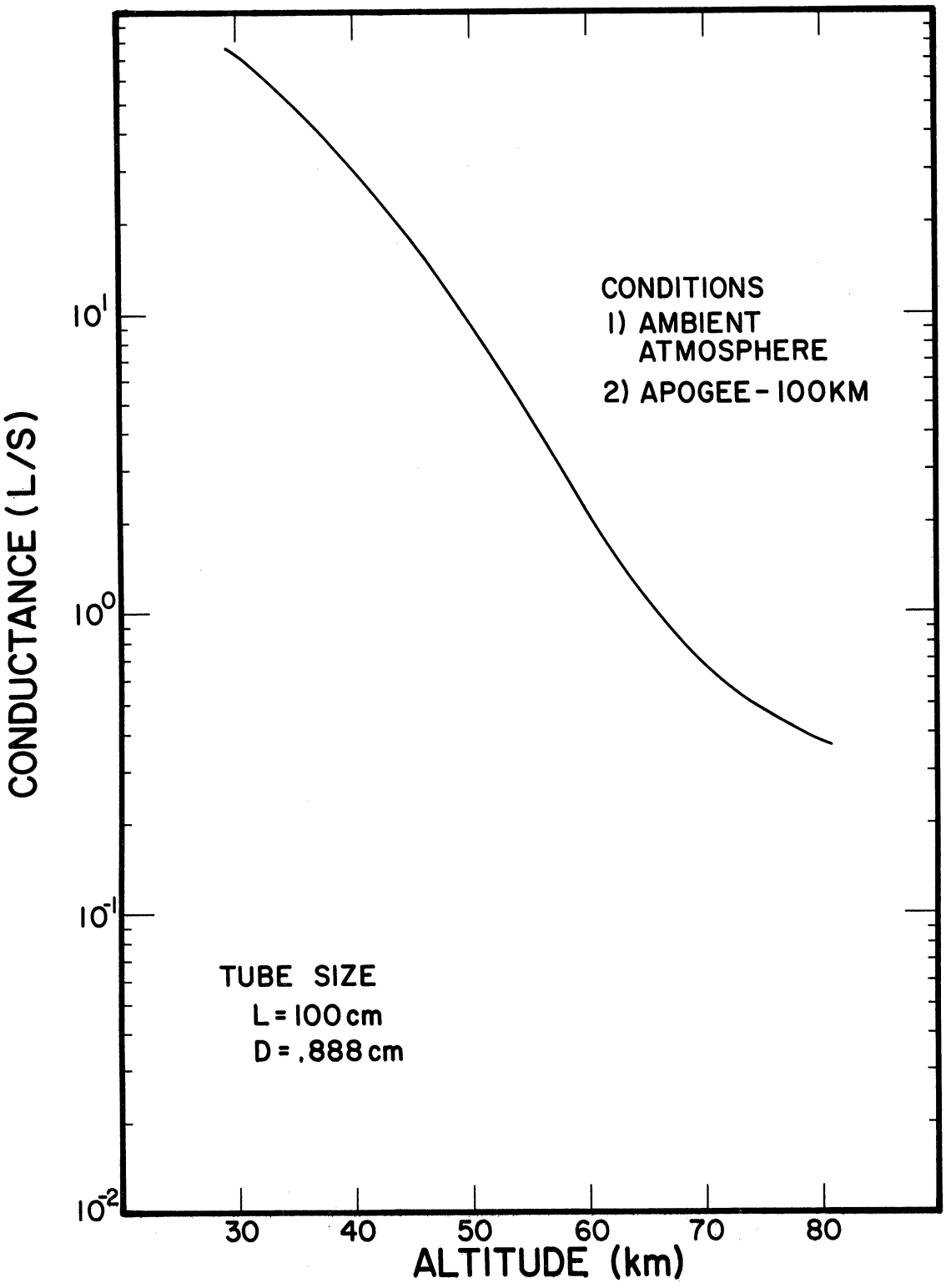

Figure 6. Tube flow rate versus altitude.

an exact calculation of the sample flow rate in the tube cannot be carried out. Our best theoretical estimate of the flow rates[25] (expressed as "ambient liters per second") that will prevail is shown in Figure 6 and for the purposes of this study the values shown are sufficiently accurate. The curve given applies to a tube whose length is 100 cm and whose diameter is approximately 0.9 cm. We see, for example, that at 30 km the flow rate will be of the order of 76 ℓ sec^{-1}, while at 80 km it will decrease to about 0.3 ℓ sec^{-1}. Since the flow rate must be known precisely in order to calculate the NO density from equation 9, the flow rates in the actual sample flow tube can be obtained experimentally. These measurements are a part of the instrument calibration procedure.

The transfer of heat from the sample to the walls of the flow tube determines the temperature of the sample when it enters the reaction chamber. The reaction rate constants k_1, k_2, k_3, and k_i are all functions of temperature[16] (generally, as the temperature increases the reaction rate increases), and, if necessary, we can use this behavior to our advantage by controlling the amount of heat lost by the sample. The two limiting cases for heat transfer are 1) adiabatic, and 2) complete accommodation. In the first case no loss of heat to the walls occurs; the sample enters the chamber at the stagnation temperature. In the second case the sample enters the reaction chamber at the chamber wall temperature. The variation with altitude of the quantity $k_1/(k_1 + k_2)$, a factor in equation 9, for these two conditions is illustrated in Figure 7. Note that at 30 km the stagnation value is approximately five times as large as the value associated with complete accommodation. This difference decreases some as the altitude increases and the stagnation temperature is lowered. At 80 km, the stagnation value is only 1.7 times as large. The ratio of the stagnation value to the accommodation value for intermediate altitudes can be determined from Figure 7. The factor k_3/k_i is assumed independent of temperature.[16]

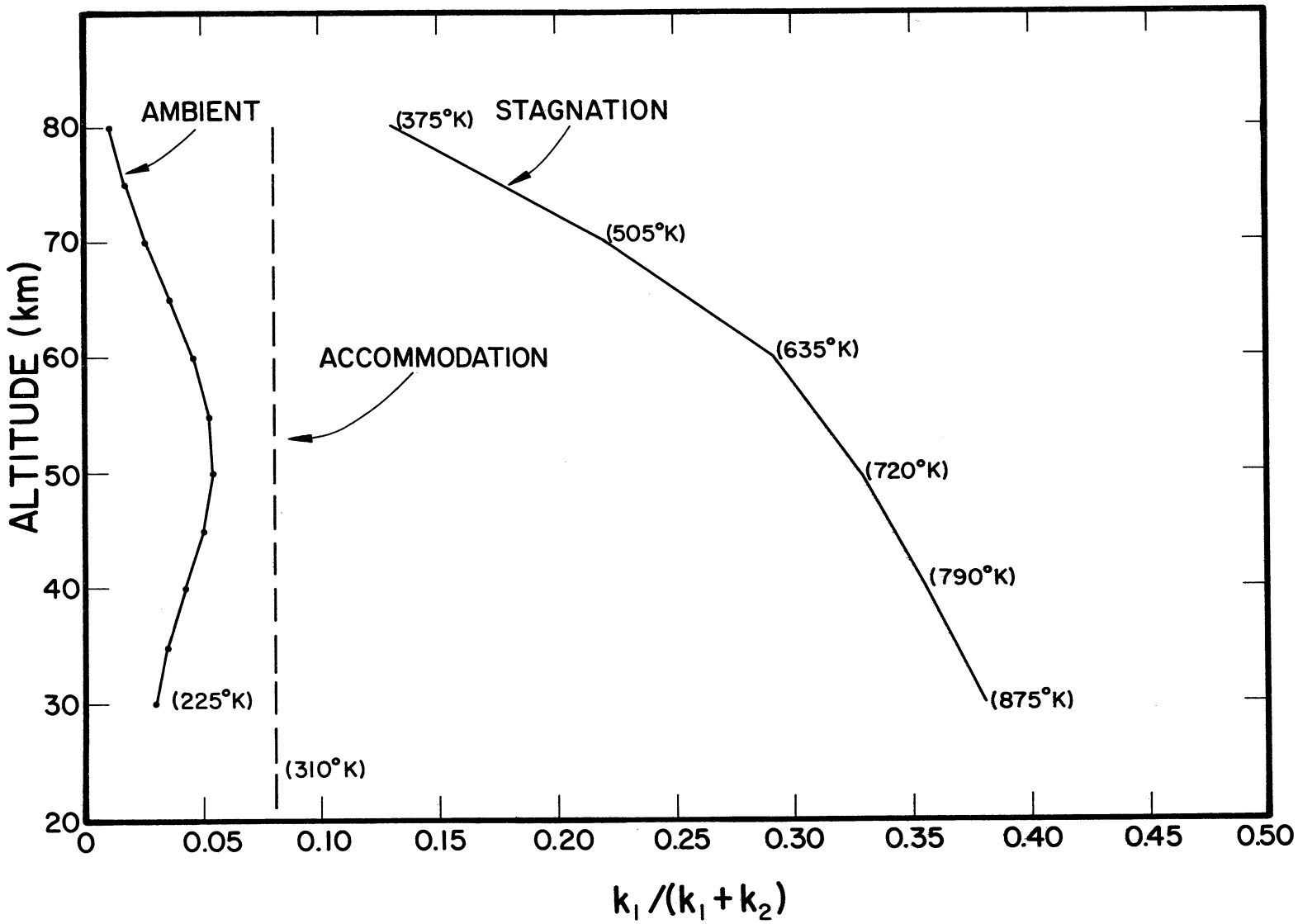

Figure 7. Temperature dependence of reaction rate constants.

All subsequent calculations are made with the assumption that complete accommodation of the sample occurs. In other words, the smallest reaction rate constants are used throughout and as a result our estimates are conservative. Figure 7 also shows the values of $k_1/(k_1 + k_2)$ if the reaction were to take place at ambient temperatures. Note that the reaction rates are enhanced by using a "hot" body such as a rocket to carry the instrument.

The helical design of the sample flow tube allows it to serve as a light trap that excludes external radiation, such as solar radiation, from the reaction chamber. The flow tube bend has a radius of curvature large enough so as not to alter the character of the flow in the tube. With respect to flow characteristics, there is no difference between this tube and a straight tube.

5.2. The Reaction Chamber

In order that the probe withstand the stresses imposed by launch, and that the chamber walls withstand oxidation by the ozone, the reaction chamber should be fabricated with stainless steel. Stainless steel is relatively impervious to attack by ozone.[26] However, it is important that as much as possible of the chemiluminescence reach the photomultiplier in order to maximize the output signal. The reflectance of stainless steel itself is not sufficient to achieve this end. But the inner walls of the chamber can be coated with a highly reflective material. The combination of reflective walls and a concave reflector, as shown in Figure 5, forms a multiple-reflecting region which serves to channel the emitted radiation to the photomultiplier. Figure 8 is a graph of the reflectance of various materials which could be used as coatings for the reaction chamber.[27] Silver has a high reflectance in the wavelength range of interest but it is readily oxidized. Since the atmosphere inside the reaction chamber will be highly oxidizing with

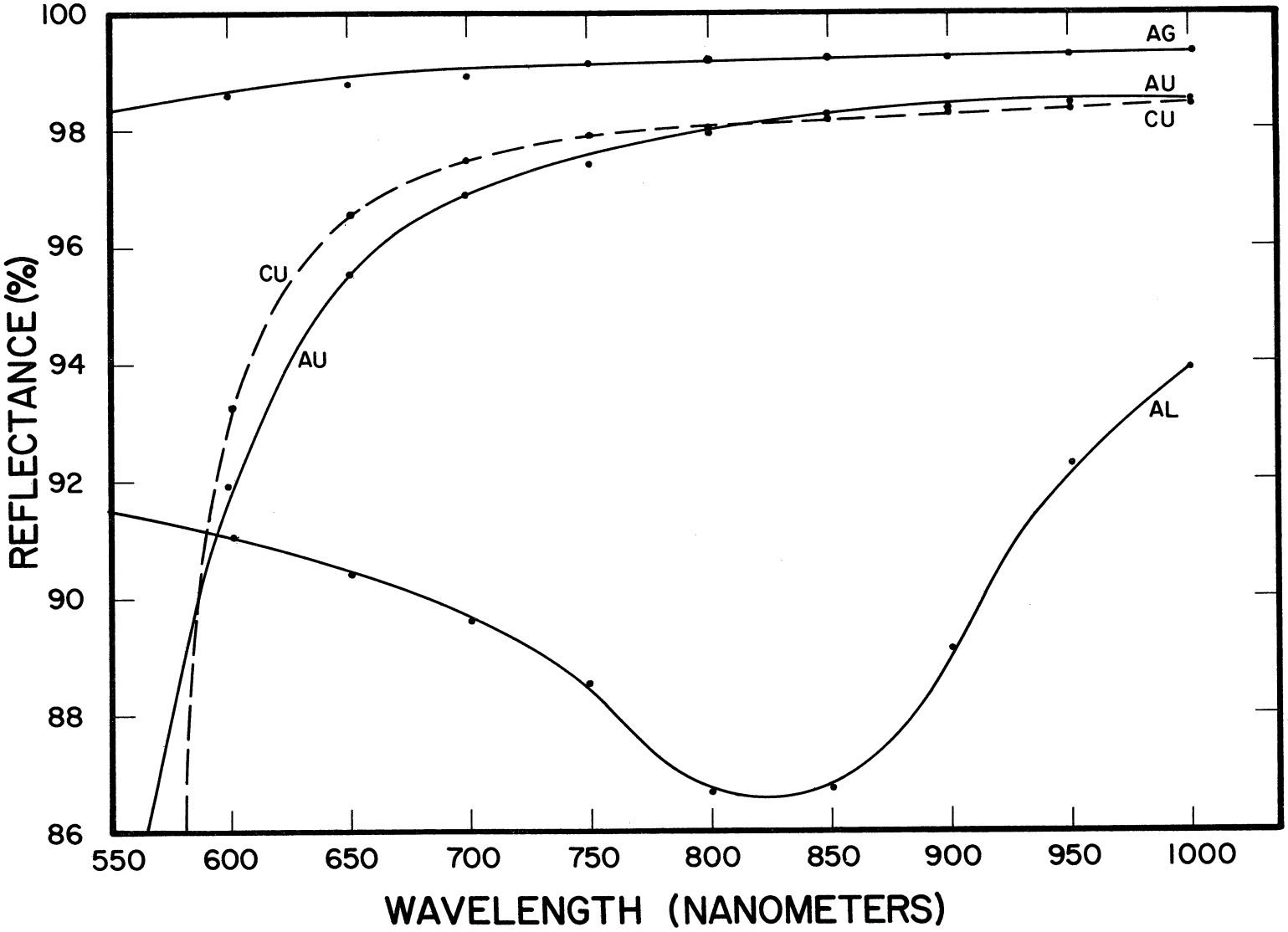

Figure 8. Reflectance of various materials.

an excess of ozone, silver could not maintain its high reflectance. Copper is also readily oxidized, and aluminum has a low reflectance. Gold is very stable in an oxidizing atmosphere and its reflectance is high over a large portion of the spectral band. Consequently, gold is a logical choice for the coating material on the inner surfaces of the reaction chamber.

The volume of the reaction chamber depends upon the concentration of ozone that can be established in it. As was noted previously (see discussion following equation 9), if a sufficiently high concentration of ozone can be introduced into the chamber, then the reaction with NO goes to completion within the volume and the total number of photons emitted is independent of the ozone concentration. However, in practice, one cannot readily generate such high ozone concentrations. In effect, we cannot ignore the exponential term in equation 9; some fraction of the nitric oxide will escape unreacted. For a constant ozone partial pressure equal to 7.5% of the total chamber pressure, Figure 9 shows the percent of unreacted nitric oxide as a function of altitude with chamber volume as a parameter. Even for a reaction volume as small as one liter, the unreacted nitric oxide is less than 5% up to 70 km. Above this altitude, the fraction of unreacted NO increases rapidly for almost any reaction volume. This loss is primarily the result of the 1/Q dependence of the exponential factor because as the vehicle slows and the ambient pressure decreases at the higher altitudes, the mass flow in the reaction vessel becomes small. However, at these altitudes, the NO concentration is increasing. As will be shown, even though significantly more than 10% of the ambient nitric oxide may escape unreacted from a one-liter chamber, the counting rate of the proposed instrument is still sufficiently high to permit easy measurement of ambient NO levels at these altitudes.

All the above considerations also apply to the sample flow

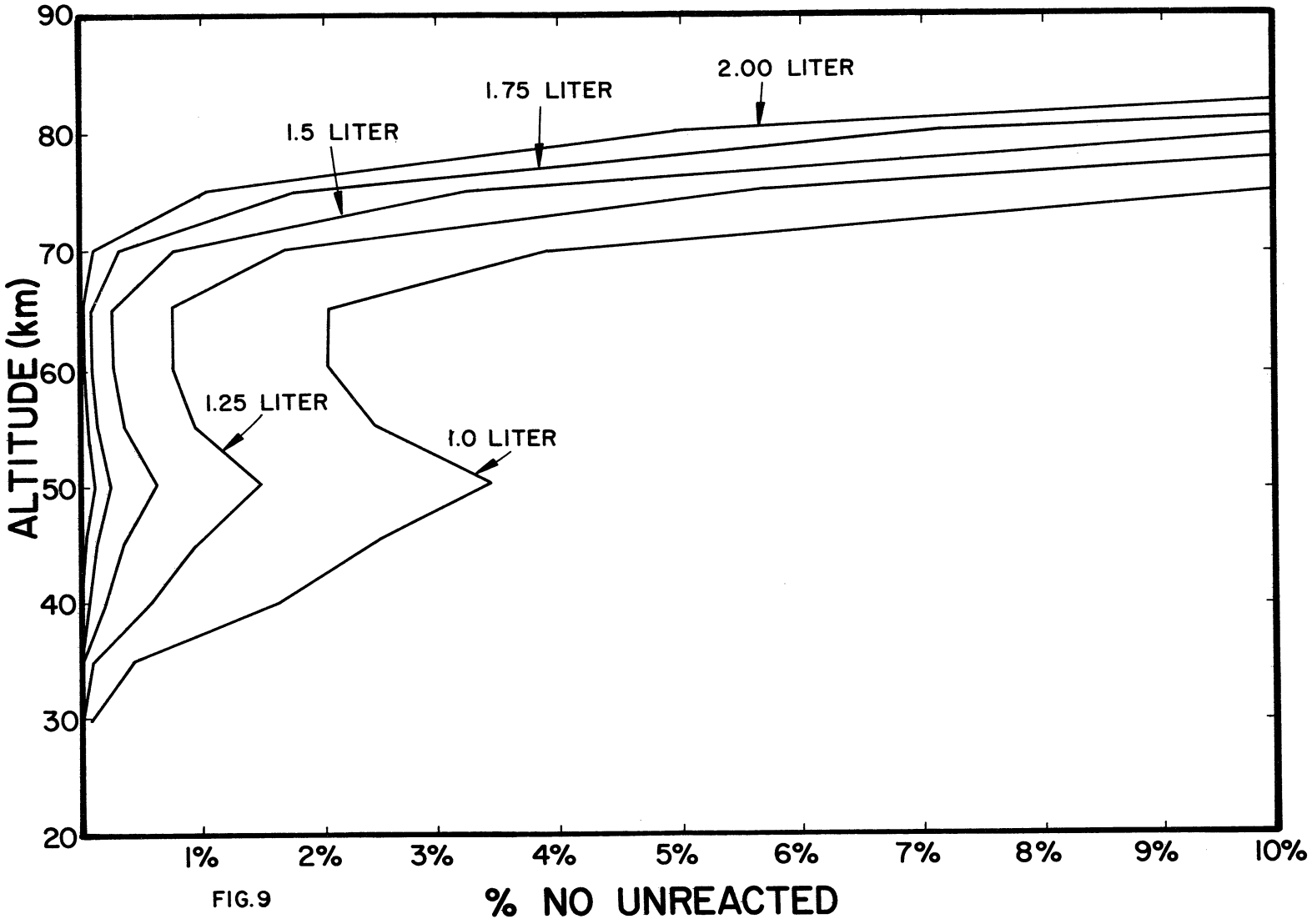

Figure 9. Percentage of unreacted NO versus altitude for several chamber volumes.

tube; it, too, is a reaction vessel because ambient ozone can react with the nitric oxide in the sample while it passes through the tube. It is important to determine if this reaction does adversely affect the NO measurement. Since the flow tube has a small diameter, the gas flow velocities will be large. As a result, the sample has a short residence time in the tube and very little nitric oxide should be destroyed. For example, if the ambient ozone concentration is 10 parts per million at 30 km, then, for the given tube parameters (a length of 100 cm and diameter of 0.9 cm, the ratio of the nitric oxide flux at the outlet to that at the inlet is 0.999. In other words, only 1 part per thousand of the ambient nitric oxide is lost because of reactions with ambient ozone in the sample flow tube. Consequently, the ambient sample is not unduly altered by this process.

5.3. The Ozone Source

Of the many ways of supplying ozone to react with ambient nitric oxide in the reaction vessel, perhaps the safest and most practical is a pressure bottle containing a mixture of ozone and freon-13. Other sources could be used but can be ruled out on the basis of either low yield, power consumption, uncertainty in ozone delivery rates, or range safety considerations. For example, a high-voltage arc discharge can be used to generate ozone; however, the power consumption and low yield makes this process unfeasible for a rocket-borne instrument. Ozone can also be adsorbed upon silica gel and subsequently driven off by heating, but the rate of evolution is always uncertain.[28]

On the other hand, the ozone-freon mixture is a standard item supplied by a reputable chemical company. It is shipped routinely to consumers in a pressured bottle maintained at dry-ice temperature. The ozone concentration is approximately 15 mole percent in the vapor phase initially.[29] In our application the stock bottle cannot be used since it is too heavy (1.6 kg)

and too large (35 cm in length, 15 cm in diameter). Instead, one can generate ozone with an ozonator, prepare a mixture with freon, and load a small bottle with the required amount of the mixture for the flight. In this way, a fresh "viable" supply of ozone is assured since, even uncooled, the ozone-freon mixture is fairly stable and will last up to a day. The bottle can be installed a few hours before firing. This procedure permits a great deal of flexibility in determining exactly how much ozone is needed, in what proportions, and at what pressure the bottle can be loaded.

If we assume that throughout the flight the total ozone-freon flow into the reaction chamber is equal to that of the sample, the chamber vents are sized so that the chamber pressure remains approximately equal to twice the ambient pressure, and the ozone concentration in the bottle is 15 mole percent, then the ozone partial pressure is 7.5% of the total. For these conditions, the total amount of ozone required for the flight is 1.7 g exclusive of any losses which may occur because of reactions with the surfaces of the ozone regulator, the walls of the ozone flow tube, etc. The amount of ozone lost in this way must be experimentally determined and the intital bottle-loading augmented to compensate for the loss. The freon-13 has no adverse effect on the system other than pressure quenching (as given by equation 4); it is completely inert with respect to the chemistry taking place in the reaction vessel.

If we assume that the sample is fully accommodated and at a temperature equal to that of the chamber walls, then, because of the temperature-dependence of the reaction rates, the ozone must be supplied at a temperature equal to that of the chamber walls also. Since gas cools upon expansion, a heat exchanger on the ozone delivery tube can be employed to warm the mixture to the chamber temperature, if necessary. Heat-sinking of the ozone flow tube to the hot parts of the skin may be all that is re-

quired to achieve this end. The ozone-freon flow can be monitored with catalytic thermocouples inserted into the ozone delivery tube.

5.4. The Photomultiplier

In the selection of a photomultiplier, we seek a tube whose spectral response overlaps a significant fraction of the emission spectrum. Most photomultipliers respond well to ultraviolet radiation. However, their sensitivities drop rapidly as wavelengths become longer until finally no significant response occurs in the infrared region beyond 900 nanometers.

For the purposes of the present discussion, we define a relative response function as the product of the quantum efficiency of a particular photomultiplier and the relative intensity of the chemiluminescent emission spectra, i.e., $R = E(\lambda) \cdot I(\lambda) d\lambda$. The units of R are quanta per unit wavelength per sec. Figure 10 compares the relative response of seven different photomultipliers.[30] The tubes are identified by their spectral response type. (Note that the curve labeled Ga-As (RCA) is scaled down by a factor of 10.) If we integrate the response curves with respect to wavelength and divide each integral by the total number N of emitted photons as calculated from equation 9, then we can define an effective yield Y which is a measure of the number of photons that yield one photoelectron,

$$Y = \frac{1}{N} \int_0^\infty E(\lambda) I(\lambda) d\lambda$$

The effective yield is a basis of comparison for photomultipliers; the greater its value, the more responsive that tube is for this application. Table 1 tabulates the effective yield for the tubes included in Figure 10.

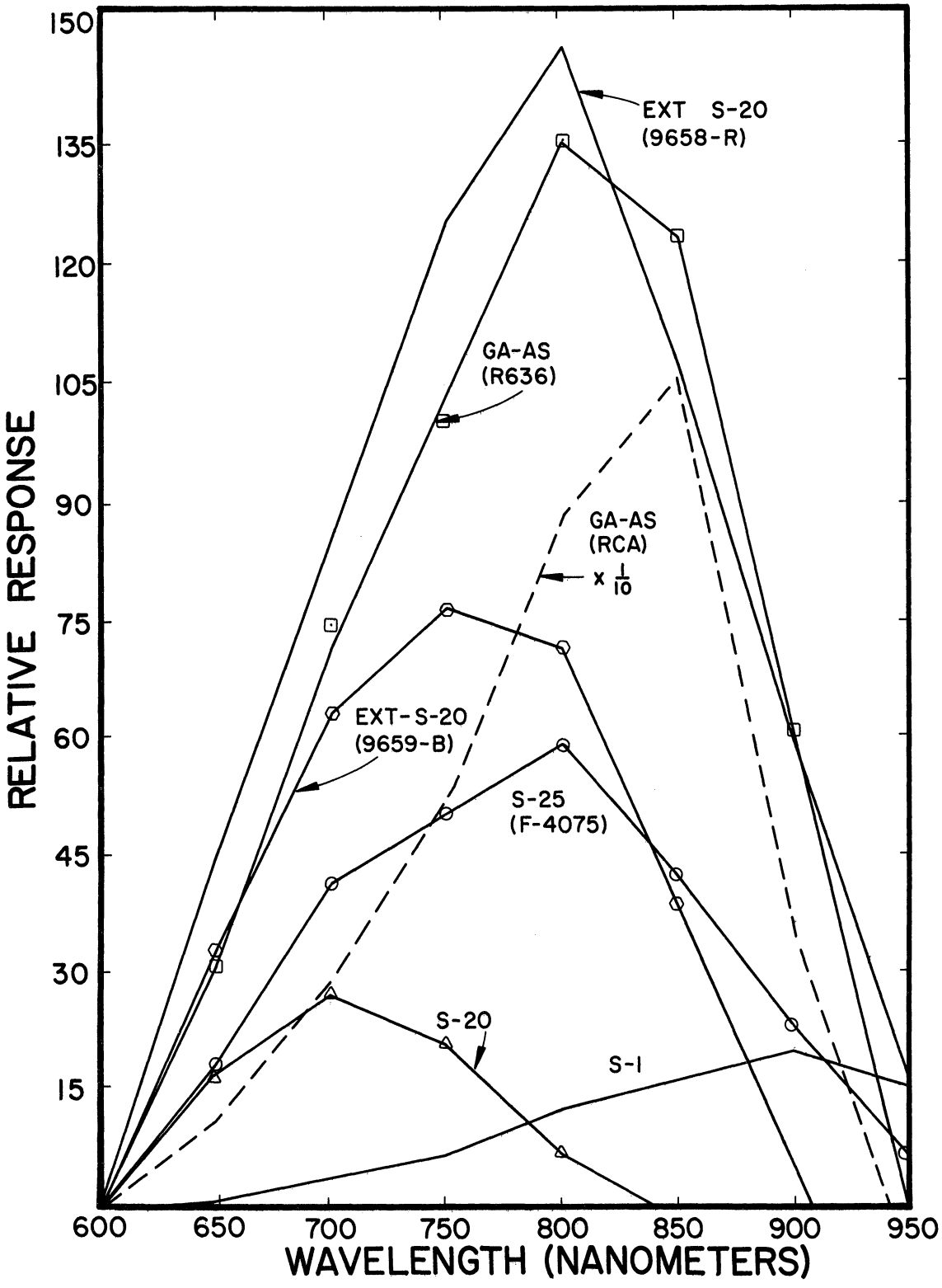

Figure 10. Relative response of seven photomultipliers versus wavelength.

TABLE 1

Photomultiplier Characteristics

Tube Type	Yield	Dark Counting Rate at 25°C (counts/cm^2-sec)
S-1	1:2800	1.5×10^6
S-20	1:3600	1.5×10^3
S-25	1:1100	1.5×10^3
EXT S-20(9659B)	1:900	7.0×10^3
Ga-As(R636)	1:500	n.a.
EXT S-20(9658R)	1:450	7.0×10^2
Ga-As(RCA)	1:100	2.5×10^4

However, relative yield is not the only factor that governs the choice of a photomultiplier. Equally important is the noise generated by the tube itself. Consequently, in addition to effective yield, the room-temperature (25°) dark counting rates[30] are also listed in Table 1. In order to reduce its dark counting rate, a photomultiplier can be cooled to dry-ice or liquid-nitrogen temperatures. However, from a practical standpoint, it is difficult to cool a tube mounted in a rocket-borne instrument. As a result, we will assume that the photomultiplier is operating in an uncooled state for all subsequent calculations.

On the basis of yield alone, the gallium-arsenide (Ga-As) tube excels; however, its dark counting rate is approximately an order of magnitude higher than the other listed tubes (with the exception of S-1). The EXT S-20R tube has the highest signal-to-noise ratio of the listed tubes, but one can effectively reduce the noise by using only a portion of the tube's photocathode. As an indication of the effectiveness of this technique, let us compare the actual dark counting rates for the two tubes, the EXT S-20R and S-25. For the former, with an effective cathode diameter of 44 mm, the dark counting rate is about 10,000 counts/sec, a good tube of this type may have a rate as low as 40,000 counts/sec.[31] On the other hand, a version of the S-25 phototube is commerically available that has built-in electrostatic focusing which reduces its effective photocathode diameter to approximately 0.1 in. (2.5 mm). As a result, the dark counting rate at 25°C is only 75 counts/sec for a typical tube and, at most, 300 counts/sec.[30] It is possible to reduce the dark counting rate of the EXT S-20R by means of a magnetic lens assembly and a thermoelectric cooler. With these accessories, the rate can be lowered by an order of magnitude. In this instance, it becomes comparable to that of the S-25. However, the added weight penalty as well as the need to provide on-stand power for the thermoelectric cooler make this solution less attractive. Thus, we conclude that the S-25 photomultiplier can achieve the highest signal-to-noise ratio in the simplest manner.

Since the low noise value cited above was obtained by using only a portion of the photocathode, it is necessary to focus the emitted radiation onto this sensitive area by some optical system. A simple system that may fill the required function is shown in Figure 5 labeled as the "VAE" cone. It is a conical, solid glass plug with a hemispherical front surface that forms the entrance aperture. All exterior surfaces with the exception of the front surface are aluminized. Multiple internal reflections "squeeze down" the incoming radiation to the diameter of the exit aperture. Such a device is presently being used on an in-house airglow experiment. Although it has been designed primarily for incoming radiation closely aligned with its axis, it can function at a reduced efficiency for radiation incident at greater angles. If such a device does not appear feasible, a proposed alternate system consists of a concave mirror with a small circular aperture at its center. This mirror works in conjunction with the concave mirror at the opposite end of the reaction chamber to form a multiple-reflecting optical system. Such systems have been to increase the efficiency of Raman tubes; with two-mirror systems nearly four-fold increases in intensity have been recorded.[32] Either of these two optical systems is a suitable alternative to a magnetic lens or thermoelectric cooler since each is a passive device, i.e., it requires no electrical power.

In order to determine the instrument response function one must estimate what fraction of the radiant energy actually falls on the phototube. Energy will be lost because of absorption at the walls, attenuation in the optical system, and reactor geometry. For the purposes of subsequent calculations, we will assume conservatively that 10% of the photons finally reach the photocathode. This number ultimately must be measured. As shown in Figure 5, the photomultiplier is positioned at the inlet end of the reaction chamber. In contrast to earlier developmental studies in which the photomultiplier was located at the opposite end, this configuration results in a higher efficiency for collecting the chemiluminescence. The Schiff instrument is con-

figured in this way.[33]

5.5. Instrument Response

The response of our hypothetical instrument is shown in Figure 11 where counting rate (in counts per sec) versus altitude is plotted for various NO profiles. Recall that we have assumed total accommodation for the incoming sample gas; it reacts with completely-accommodated ozone at the temperature of the chamber walls. Also, as stated above, we assume that only 10% of the chemiluminescent radiation reaches the photomultiplier. As a result, the counting rates given here are conservative estimates.

Profile I in the Figure 11 is the counting rate based on our derived NO profile which incorporates Ridley's upper and lower bounds. At 30 km the value corresponding to his upper bound is approximately 2×10^5 counts/sec. This rate rises to a maximum of about 6×10^5 counts/sec at 45 km and then falls to about 1.5×10^4 counts/sec at 80 km. If Ridley's lower bound is used, then the counting rate is 3.5×10^4 counts/sec at 30 km.

Counting rates independent of assumed profiles can be obtained from the mixing-ratio lines of Figure 4. Recall that the lowest line was for a mixing ratio of 1 part per billion. If this rate is constant with altitude, then the counting rate shown by the lowest dashed line in Figure 11 results. In a similar way, the middle and upper dashed lines of Figure 4 are for mixing ratios of 10 parts per billion and 100 parts per billion, respectively.

Natural limits to the counting rate exist at both ends of the scale. An upper bound is set by the circuitry; counting rates greater than 6×10^6 counts/sec are hard to achieve. The lower bound is set by the dark counting rate; in this instance, a conservative estimate of 600 counts/sec is indicated. Thus, counting rates between 6×10^2 to 6×10^6 counts/sec are acceptable. In conjunction with these bounds, we see that the

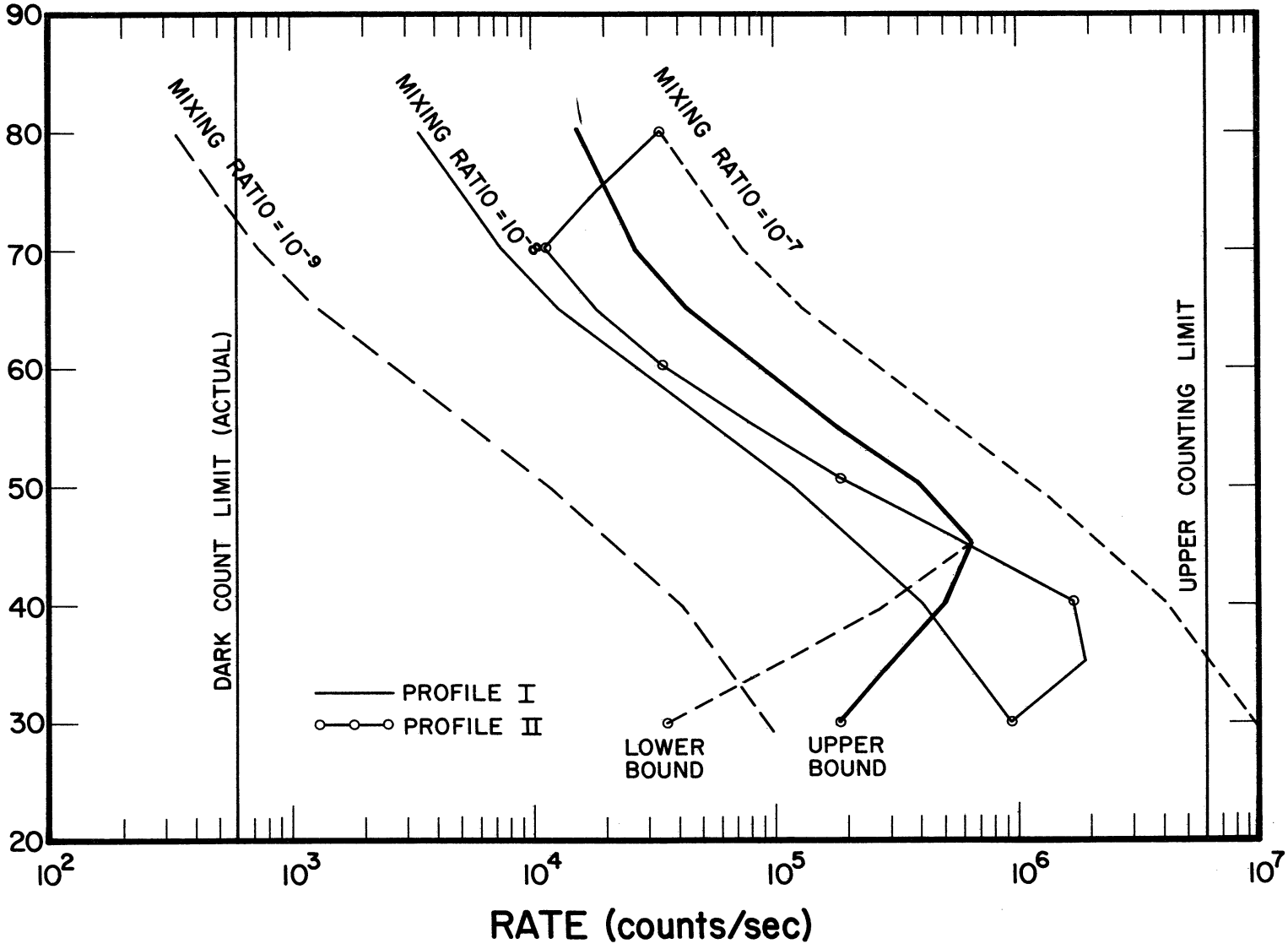

Figure 11. Counting rate versus altitude for various NO profiles.

proposed instrument can readily detect and measure nitric oxide levels at 1 part per billion in the altitude range from 30 to 73 km. At the other extreme, a concentration of 100 parts per billion can be measured between 35 and 80 km, as given by the upper dashed curve.

6. CONCLUSION

In conclusion, we find that a chemiluminescent nitric oxide detector carried aloft by a rocket is feasible. Its ultimate sensitivity and dynamic range is such that nitric oxide concentrations in the altitude interval from 30 to 80 km can be successfully measured. Although there are some technical problems, these can be solved without exceeding the state-of-the-art.

7. REFERENCES

1. Reid, G., J. Geophys. Res., 75, 2551, 1970.

2. Strobel, D. F., J. Geophys. Res., 77, 1337, 1972.

3. Strobel, D. F., J. Geophys. Res., 76, 2441, 1971.

4. Working Group 11 on Ion Chemistry of the D and E Regions, Conclusions of Ad Hoc Panels Convened at Urbana Meeting, STP Notes, 13(69), 1969.

5. Sechrist, C. F., Jr., J. Atmos. Terr. Phys., 29, 113, 1967.

6. Geisler, J. L., and R. E. Dickinson, J. Atmos. Terr. Phys., 30, 1505, 1968.

7. Christie, A. D., J. Atmos. Terr. Phys., 32, 35, 1970.

8. Gregory, J. B., and A. H. Manson, J. Atmos. Terr. Phys., 31, 703, 1969.

9. Geller, M. A., and C. F. Sechrist, Jr., J. Atmos. Terr. Phys. 33, 1027, 1971.

10. Bowhill, S. A., Ion Chemistry of the D and E Regions—— A Survey for Working Group 11 of the Inter-Union Commision on Solar-Terrestrial Physics, STP Notes, 20(68), 1968.

11. Bowhill, S. A., Program Document for Neutral and Ion Chemistry, April 10, 1972.

12. Barth, C. A., Ann. Geophys. 22, 198, 1966.

13. Pearce, J. B., J. Geophys. Res., 74, 853, 1969.

14. Meira, L. G., J. Geophys. Res., 76, 202, 1971.

15. Working Group 11 on Ion Chemistry of D and E Regions, Program Recommendations, STP Notes, 14(69), 1969.

16. Clough, P. N., and B. A. Thrush, Trans. Faraday Soc., 63, 915, 1967.

17. Fontijn, A., A. J. Sabadell, and R. J. Ronco, Anal. Chem., 42, 575, 1970.

18. Stuhl, F., and H. Niki, Scientific Research Staff Report, Ford Motor Company, 1970.

19. Stedman, D. H., E. E. Daby, F. Stuhl, and H. Niki, J. Air Poll. Control Assoc., 22, 260, 1972.

20. Ridley, B. A., H. I. Schiff, and K. H. Welge, Centre for Research in Experimental Space Science Report, York University, 1972.

21. Ridley, B. A., private comm.

22. Nicolet, M., J. Geophys. Res., 70, 691, 1965.

23. Nicolet, M., J. Geophys. Res., 70, 679, 1965.

24. Stolarski, R.S., and R. J. Cicerone, Trans. AGU, 54 (SA17), April 1973.

25. Horvath, J., private comm.

26. Encyclopedia of Chemical Technology.

27. American Institute of Physics Handbook.

28. Ozone Chemistry and Technology, Americal Chemical Society, 1959.

29. General Catalog, Matheson Gas Products.

30. Manufacturer's literature.

31. Lieberman, L. E., private comm.

32. Welsh, H. L., Cumming, C., and Stansbury, E. J., J. Optical Soc. America, 41, 712, 1951.

33. Ridley, B. A., K. H. Welge, H. I. Schiff, L. R. Megill, and A. W. Shaw, Second Conf. on CIAP, U.S. Dept. of Transportation, 146, 1972.

UNIVERSITY OF MICHIGAN
3 9015 03125 9115